Surface-acoustic-wave propagation in paramagnets

C. Lingner and B. Lüthi
Physikalisches Institut der Universität, Robert-Mayer-Str. 2–4, D-6000 Frankfurt a.M., Federal Republic of Germany
(Received 1 July 1980)

We have investigated propagation of surface-acoustic waves SAW in the paramagnetic phases of $CeAl_2$ and SmSb. The temperature dependence of the SAW velocity is well accounted for with a magnetoelastic coupling of the strain components to the crystal-field-split magnetic ions. In $CeAl_2$ we found large magnetic field effects on the Rayleigh wave velocity at 4.3 K which can be qualitatively explained by the same magnetoelastic coupling. Contributions to the SAW velocities from rotationally invariant magnetoelastic interactions could be determined. In $CeAl_2$ we found evidence for the magnetoacoustic analog of the Cotton-Mouton-Voigt effect for the SAW. It manifests itself as an amplitude modulated interference effect which we can qualitatively account for. This is the first time Rayleigh waves have been used to investigate the various analogous magnetoelastic effects known from previous acoustic bulk wave experiments.

I. INTRODUCTION

Surface acoustic waves (SAW) are very important for different devices.[1] However, their use for the study of physical properties of materials has been limited. There are experimental and theoretical investigations of SAW attenuation,[2] applications of SAW for the study of proximity effects in superconductors,[3] and SAW experiments using Brillouin scattering techniques.[4] However, SAW velocity experiments are scarce.[5]

In this paper we present a thorough study of SAW propagation in single-crystal paramagnets. We give experimental results for the two cubic rare-earth intermetallic compounds SmSb and $CeAl_2$. These materials exhibit anomalous elastic bulk properties, making them a good test case for a study of SAW propagation. Their magnetic and elastic properties have been studied extensively before.[6,7] This enables us to make a quantitative study of SAW properties.

We present experimental results on the temperature and magnetic field dependence of the SAW velocity in these compounds together with a quantitative analysis. We also present the first magnetoacoustic birefringence effects observed with SAW. A detailed theoretical investigation of SAW velocities has been given before.[8]

In the next sections we discuss experimental details and a calculation of the SAW velocity using the magnetoelastic coupling of macroscopic strains to the rare-earth ions. In the following sections we present experimental results and discussions on the temperature and magnetic field dependence of the SAW velocity.

The main results of our study are the following: as for bulk waves, SAW exhibit crystal-field effects which can be quantitatively described with the appropriate strain susceptibilities. In the magnetically ordered region strong domain-wall stress effects are also effective for SAW. The magnetic field dependence of SAW velocities exhibits pronounced effects which can be interpreted as for bulk waves. Contributions due to rotationally invariant magnetoelastic interactions can be isolated also for SAW. The magnetoacoustic analog of the Cotton-Mouton-Voigt birefringence effects, observed previously for bulk waves,[7] has been observed also for SAW in $CeAl_2$ as an interference effect.

II. EXPERIMENTAL

The SAW are generated by using piezoelectric CdS transducers. The transducer films of about 4μ thickness were either rf sputtered or vapor deposited by the method described by de Klerk and Kelly.[9] We produced the two films simultaneously near the corners of the highly polished crystal surface to ensure identical performance. On top of these films we evaporated comblike Al electrodes (single-phase array) via photoetched masks. The complete arrangement is shown schematically in Fig. 1, together with typical dimensions. The principle of operation of these SAW transducers has been described earlier. An excellent review can be found in *Physical Acoustics*.[10]

We investigated two crystals, $CeAl_2$ and SmSb. The propagation direction of the SAW was [100] for $CeAl_2$ and [110] for SmSb. The frequencies used were in the range of 9 to 25 MHz. In the $CeAl_2$ case we were able to observe the first overtone of the fundamental frequency. The measurements of the veloc-

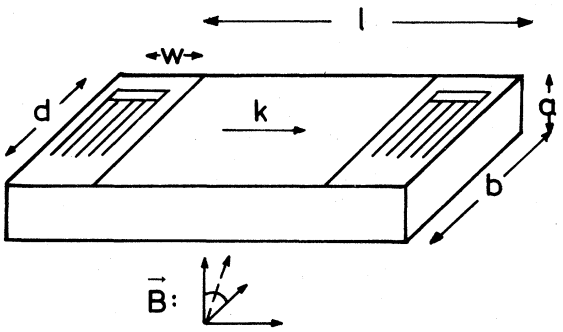

FIG. 1. Crystal with SAW transducers. Typical dimensions: $l = 10$ mm; $a = 4$ mm; $b = 6$ mm; $d = 4$ mm; and $W = 2$ mm. Also indicated are the magnetic field directions used in our experiments.

ity as a function of temperature in the range of 300 to 2 K and as a function of an external magnetic field at 4.3 K were performed using our standard phase-comparison system.[11] A typical sensitivity was 1 part in 10^5. The high magnetic field up to 12 T was generated by a superconducting coil (Intermagnetics Corp.). The various magnetic field directions used in our experiments are also shown in Fig. 1. The accuracy of field alignment was better than 3°.

The absolute sound velocity could be determined with different methods: (i) from the distance of the electrodes and the transit time of the SAW pulse; (ii) from the generating frequency and the distance between adjacent comb lines of the electrodes; and (iii) from reflections at the surface corners, i.e., travel time of the pulse from the receiving transducer to the corner and back and the appropriate distances. All three methods gave results in good agreement with each other. One difficulty, however, arises from the extended electrode structure which cannot be neglected compared to the length of the free surface. As a result, we could not determine the absolute SAW velocity better than ±5%. Within these limits it also agrees with the calculated velocity using the known bulk elastic constants. Because of the rather large inaccuracy we give only relative SAW velocity changes $\Delta v/v$ as a function of temperature or magnetic field in Figs. 2 to 5. Both the sputtered and the vapor deposited films gave the same results; the sputtered films, however, showed a better efficiency. For the amplitude modulation in the Cotton-Mouton geometry we used a boxcar receiving system for the direct SAW pulse or the first reflection from the corner.

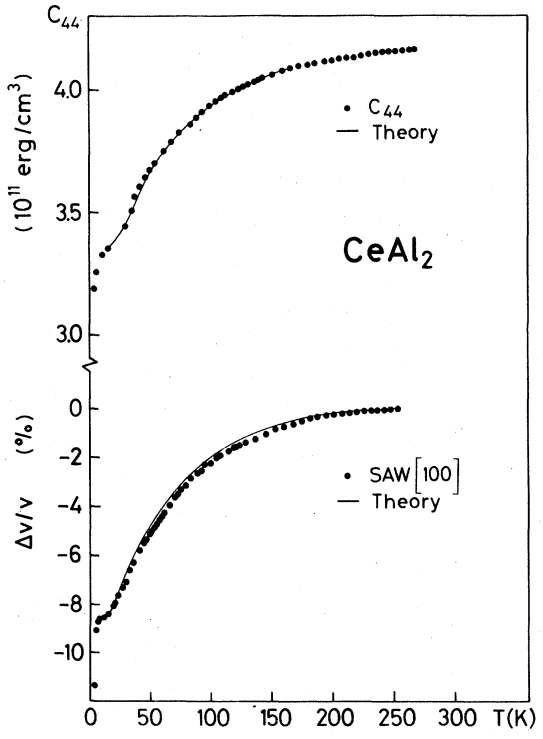

FIG. 2. Temperature dependence of SAW velocity in $CeAl_2$ for $\vec{k} \parallel [100]$. The theory is given by the full line. For comparison $c_{44}(T)$ is given in the upper part of the figure (from Ref. 7).

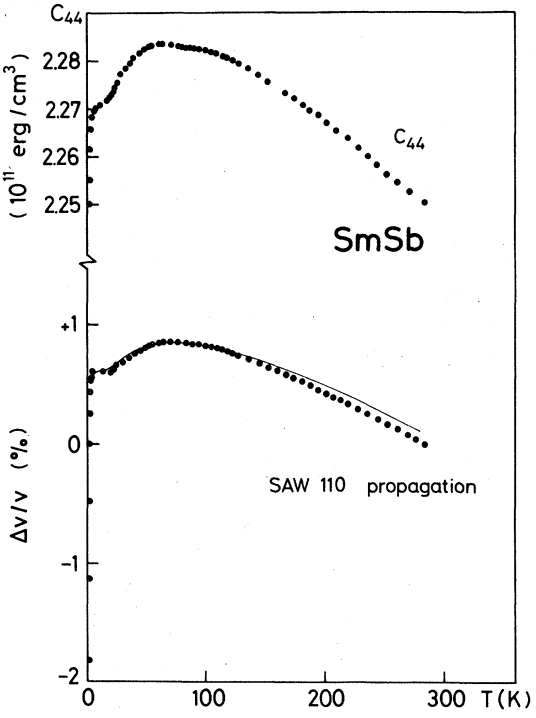

FIG. 3. Temperature dependence of SAW velocity in SmSb for $\vec{k} \parallel [110]$. The theory is given by the full line. For comparison $c_{44}(T)$ is given in the upper part of the figure (from Ref. 6).

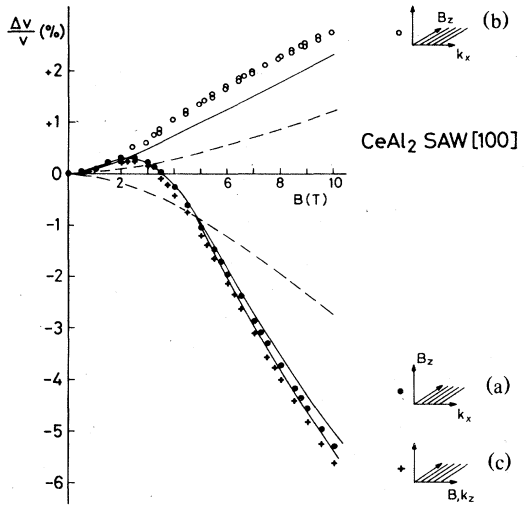

FIG. 4. Magnetic field dependence of SAW velocity of $CeAl_2$ at 4.3 K for different orientation of k, B with respect to the surface. $\vec{k} \parallel [100]$. Dotted lines are calculated using Eq. (4). Full lines are calculations using Eqs. (1) and elastic constants from Ref. 7.

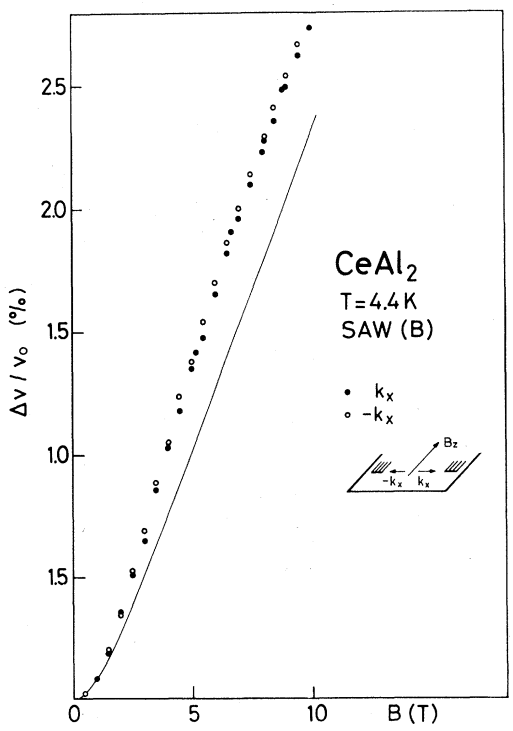

FIG. 5. Magnetic field dependence of SAW velocity of $CeAl_2$ at 4.4 K for geometry (b) with $\vec{B}$, $\vec{k}$, and $-\vec{k}$ as given in the inset. Full line is the same as in Fig. 4.

III. THEORY

A treatment of SAW, the so-called Rayleigh waves, for isotropic media using elastic continuum theory can be found in standard texts.[12] The case for elastic anisotropic media, especially cubic crystals, has also been given before.[13] For the equation of motion

$$\rho \ddot{u}_i = \sum_j \frac{\partial \sigma_{ij}}{\partial x_j}$$

one has the boundary condition for the stress tensor components $\sigma_{in} = 0$ for the free surface of the material, with $\vec{n}$ denoting the normal direction to the surface. Using for the displacement $\vec{u}$ the ansatz

$$\vec{u} = \vec{U} e^{-\kappa x_n} e^{i(\vec{k}\cdot\vec{x}-\omega t)}$$

one obtains a cubic equation[13] for the ratio $R = \rho v^2 / c_{11}$ (v being the SAW velocity):

$$\left(1 - \frac{c_{11}}{c_{44}} R\right)\left(1 - \frac{c_{12}^2}{c_{11}^2} - R\right)^2 = R^2(1-R) \ , \qquad (1a)$$

for [100] propagation and

$$\left(1 - \frac{c_{11}}{c_{44}} R\right)\left(\frac{c_L}{c_{11}} - \frac{c_{12}^2}{c_{11}^2} - R\right)^2 = R^2\left(\frac{c_L}{c_{11}} - R\right) \ , \qquad (1b)$$

for [110] propagation. The [100] and [110] directions are the propagation directions investigated in our experiments. c_{ij} are the bulk elastic constants with $c_L = \frac{1}{2}(c_{11} + c_{12} + 2c_{44})$. As will be shown below (Figs. 2 and 3), Eqs. (1) describe the temperature dependence of the SAW velocity very well.

For studying magnetoelastic effects with SAW we use an interaction Hamiltonian, coupling the strain components ϵ_{ij} to the rare-earth ion which is characterized by the angular momentum operator $\vec{J}$. We are interested only in single-ion effects in the paramagnetic region. Then the magnetoelastic Hamiltonian has the usual form for cubic crystals[14,15]

$$H_{me} = -g_2 N(\sqrt{3}\epsilon_2 O_2^2 + \epsilon_3 O_2^0) - 2g_3 N(\epsilon_{xy} O_{xy} + \epsilon_{xz} O_{xz} + \epsilon_{yz} O_{yz}) \ . \qquad (2)$$

Here ϵ_2 and ϵ_3 denote the strain with Γ_3 symmetry $O_2^2 = J_x^2 - J_y^2$, $O_2^0 = 2J_z^2 - J_x^2 - J_y^2$, and $O_{ij} = J_i J_j + J_j J_i$. g_2 and g_3 are magnetoelastic coupling constants which are known for SmSb and $CeAl_2$ from bulk elastic measurements.[6,7] N is the number of identical magnetic ions per unit volume.

We can generalize Eqs. (1) by calculating additional contributions to the stress tensor from the magnetoelastic interaction. In a concise way we can write for a stress component of symmetry Γ

$$\sigma_\Gamma = c_\Gamma^0 \epsilon_\Gamma + g_\Gamma \langle O_\Gamma \rangle N = \epsilon_\Gamma (c_\Gamma^0 + g_\Gamma^2 N \chi_\Gamma) \ , \qquad (3)$$

where χ_Γ is the single-ion strain susceptibility and c_Γ^0 the corresponding background elastic constant. The further calculation then proceeds as outlined for the results of Eqs. (1). For the different geometries with

respect to propagation direction $\vec{k}$ of the SAW and the magnetic field $\vec{B}$ we get the corresponding equation to Eqs. (1) ($\vec{k}$ always along a cubic axis):

$$\left[1-\frac{\tilde{c}_{11}}{\tilde{c}_{44}}R\right]\left[1-\frac{c}{\tilde{c}_{11}}-\frac{\tilde{c}_{12}^2}{\tilde{c}_{11}^2}-R\right]^2=R^2\left[1-\frac{c}{\tilde{c}_{11}}-R\right], \tag{4}$$

where the c, $\tilde{c}_{ij}$ are renormalized elastic constants which can be expressed by the strain susceptibilities $\chi(O_\Gamma)$. We have investigated three geometries: (a) surface in (x,y) plane $\vec{k}=(k_x,0,0)$, $\vec{B}=(0,0,B_z)$ $\tilde{c}_{11}=c_{11}-\frac{2}{3}g_2^2N\chi(O_2^0)$, $\tilde{c}_{12}=c_{12}+\frac{1}{3}g_2^2N\chi(O_2^0)$, $\tilde{c}_{44}=c_{44}-g_3^2N\chi(O_{xz})$, and $c=\frac{1}{2}g_2^2N[3\chi(O_2^2)-\chi(O_2^0)]$; (b) surface in (x,z) plane $\vec{k}=(k_x,0,0)$, $\vec{B}=(0,0,B_z)$ $\tilde{c}_{11}=c_{11}-\frac{1}{2}g_2^2N[3\chi(O_2^2)+\frac{1}{3}\chi(O_2^0)]$, $\tilde{c}_{12}=c_{12}+\frac{1}{2}g_2^2N[3\chi(O_2^2)-\frac{1}{3}\chi(O_2^0)]$, and $\tilde{c}_{44}=c_{44}-g_3^2N\chi(O_{xy})$, $c=0$; and (c) surface in (y,z) plane $\vec{k}=(0,0,k_z)$, $\vec{B}=(0,0,B_z)$ $\tilde{c}_{11}=c_{11}-\frac{1}{2}g_2^2N[3\chi(O_2^2)+\frac{1}{3}\chi(O_2^0)]$, $\tilde{c}_{12}=c_{12}+\frac{1}{3}g_2^2N\chi(O_2^0)$, $\tilde{c}_{44}=c_{44}-g_3^2N\chi(O_{xz})$, and $c=-\frac{1}{2}g_2^2N[3\chi(O_2^2)-\chi(O_2^0)]$. Equation (4), together with the renormalized elastic constants for the three geometries, determines the propagation of the SAW as a function of temperature and magnetic field. We shall see in the section on results that the most important contribution arises from the c_{44} mode which depends on the various $\chi(O_{ij})$ for the different geometries. Note that the additional term c is zero for $B=0$, because $3\chi(O_2^2)=\chi(O_2^0)$ for $B=0$ by symmetry and Eq. (4) reduces to Eqs. (1) in this case. However, $\chi(O_\Gamma)$ does not disappear for $B=0$, because these strain susceptibilities give the anomalous temperature dependence for both bulk waves[14] and SAW. In our treatment we have neglected terms involving antisymmetric strains, which are needed to ensure rotational invariance of the magnetoelastic Hamiltonian.[16] These terms have been taken into account in a full theoretical treatment of the same problem.[8] From experiments testing rotational invariance in rare-earth compounds, one notices[7,17] that these terms give effects of the order of 1% of the total magnetic-field-dependent effect. We shall comment on these effects and determine them when we present our results.

IV. RESULTS AND DISCUSSION

First we present results on the temperature dependence of SAW velocities and afterwards on the magnetic field dependence. Finally we comment on magnetoacoustic birefringence effects.

A. Temperature dependence of SAW velocities

In Figs. 2 and 3 we give experimental results on SAW velocities for $CeAl_2$ and SmSb. The propagation direction is [110] for SmSb and [100] for $CeAl_2$. Also shown in the figures are the corresponding c_{44} modes. Both the Sm^{3+} and Ce^{3+} ions have $J=\frac{5}{2}$ which splits in the cubic crystal field into a Γ_7 doublet ground state and an excited Γ_8 quartet state. The splitting is 65 K for SmSb (Ref. 6) and 90 K for $CeAl_2$.[7] Therefore the temperature dependence of both c_{44} and SAW velocity is the same in the two cases. SmSb and $CeAl_2$ have magnetic phase transitions at 2.11 and 3.8 K, respectively. One notices for both the c_{44} mode and the SAW a very strong softening in the antiferromagnetic phases due to domain-wall stress effects.

The temperature dependence of c_{44} for these cases has been discussed before.[6,7] The strain-magnetic ion coupling for the crystal-field-split rare-earth ion, which gives rise to the strain susceptibility, explains this effect very well, as well as many other cases.[14] A fit of Eqs. (1) or (4) can equally well explain the temperature dependence of the SAW velocities. This means that an analogous crystal-field effect is also present for the SAW. This is not surprising because for our measuring frequencies of 9 to 25 MHz the penetration depth $1/\kappa$ is about 0.2 mm. If one calculates the particle displacements in the SAW one finds for most of the penetration region a long axis parallel to the surface normal. This implies a strong relation to the c_{44}-type bulk mode. Indeed if one considers the relative contributions to the SAW velocity from Eqs. (1) or (4) one finds a 85% contribution from c_{44} and only a 15% contribution from the other modes c_{11} and c_{12}. This explains the similar temperature dependence of the SAW velocities and the corresponding c_{44} modes for SmSb and $CeAl_2$. As seen from Figs. 2 and 3 the temperature dependence of the SAW velocities in the paramagnetic region agrees very well with the one calculated from Eq. (4) using known magnetoelastic coupling constants.[6,7] Since the bulk elastic modes are also very well explained with this magnetoelastic coupling[6,7,14] one can likewise take Eqs. (1) with the measured bulk constants c_{ij}, giving the same good agreement.

As for the case of bulk elastic waves the strong softening of the SAW velocity for $T<T_N$ can be accounted for by a domain-wall stress effect. This softening amounts to 5% from T_N to 1.8 K for the case of SmSb. This result implies that domain walls are effective scatterers for SAW, which results also in a strong observed damping of these waves. It would be interesting to study the interaction of SAW and domain walls under well defined conditions.

B. Magnetic field dependence of SAW velocities

In Fig. 4 we show the magnetic field dependence of the SAW velocities in $CeAl_2$ at 4.3 K for the three modes discussed in the theory Sec. III [Eq. (4)]. One notices a similar behavior for cases (a) and (c) in-

volving the strain susceptibility $\chi(O_{xz})$, namely, a negative change for $\Delta v/v$ for high fields and a positive change for $\Delta v/v$ for case (b) involving the strain susceptibility $\chi(O_{xy})$. A similar behavior was found for the c_{44} mode in $CeAl_2$ as seen in Fig. 2 of Ref. 7. It was shown there that the opposite sign of $\chi(O_{xz})$ and $\chi(O_{xy})$ is due to the symmetry-breaking field B, changing c_{44} to a c_{66}-like mode for the case involving $\chi(O_{xy})$. Similar arguments can be given for the SAW if one considers the particle displacements for the three cases. Here (a) and (c) have particle displacements in the (x,z) plane whereas for case (b) it is in the (x,y) plane.

One can interpret the results of Fig. 4 quantitatively. Using Eq. (4) for the three different cases (a), (b), and (c) with the known coupling constants[7] $|g_2| = 71$ K/ion and $|g_3| = 270$ K/ion one obtains the two dotted curves given in Fig. 4, where cases (a) and (c) are almost degenerate. While it gives qualitatively correct results, it explains only 50% of the measured effect. We notice the same discrepancy as for the case of bulk c_{44} waves.[7] This discrepancy must be due to the vicinity of the magnetic phase transition, where the single-ion strain susceptibility cannot explain the whole effect, and fluctuation effects must play an important role. For $CeAl_2$ the magnetoelastic coupling constant g_3 is much larger than g_2. The reason for this was discussed before.[7] It means that the important contributions to the SAW velocity come from the renormalized c_{44} elastic constant as noticed above in the case of the temperature dependence of SAW. Therefore the full curves in Fig. 4 are SAW velocities using the magnetic field dependence of the different c_{44} modes from Fig. 2 of Ref. 7. One notices a rather close agreement with the measured SAW velocities for the three geometries in Fig. 4. The main features in Fig. 4 have been explained successfully using the expressions derived in the theory Sec. III. One noticeable lack of agreement is the small difference observed for the cases (a) and (c) and the almost degenerate theoretical results (dotted curve in Fig. 4). The contributions due to $\chi(O_2^2)$ and $\chi(O_2^0)$ for the SAW velocities are too small to give the observed splitting. This splitting is due to rotationally invariant magnetoelastic interactions, observed in $CeAl_2$ before,[7] which have not been taken into account in our theory. They will be discussed below. In SmSb we could not find any magnetic field effect on the SAW velocity at 4.3 K. This agrees with the experimental results obtained by bulk measurement.[6] A magnetic field effect on the bulk velocity was found only at temperatures below T_N.

C. Rotationally invariant magnetoelastic interaction

As pointed out above, the theory developed in Sec. III does not involve antisymmetric strain components ω_{ij} and is based on a magnetoelastic Hamiltonian [Eq. (2)] which does not fulfill the requirement of rotational invariance. Such effects for rare-earth systems have been discussed previously both experimentally[7,14,17] and theoretically.[15,16] A theory including such effects for SAW has recently been developed.[8]

We discuss two experimental features due to rotational invariance. The first is noticeable in Fig. 4 and was already mentioned in the previous section. The different magnetic field dependence of cases (a) and (c) in Fig. 4 cannot be explained with our theory given above. The experimental curves for the two geometries correspond directly to the two c_{44} modes of Fig. 2 in Ref. 7, from which one can determine the rotationally invariant magnetoelastic contributions. The splitting of the two modes of Fig. 4 in our paper and the corresponding splitting of the c_{44} mode in Ref. 7 have the same relative order of magnitude. This is also borne out in the complete calculation of Ref. 8. In the case of c_{44} in $CeAl_2$ the magnitude of this effect was well accounted for.[7] The similar size of this effect for SAW shows that this is also true for the case under consideration.

Another effect which should occur at a surface was proposed in Ref. 8 by a symmetry argument. It was suggested that for the geometry in case (b) discussed above, the magnetic field dependence of the SAW velocity should depend on the direction of k_x and B_z. That is to say that (k_x,B_z) should give a different effect than $(-k_x,B_z)$. Figure 5 shows our result for this geometry. In the measured frequency range of 9 to 25 MHz we did not observe any such geometrical dependence within the accuracy of our field alignment of about 3°. Any such dependence should be only observable at higher frequencies.[8]

D. Magnetoacoustic birefringence experiments

Magnetoacoustic birefringence effects (Faraday- and Cotton-Mouton-Voigt effect) have been observed in ferrimagnets and antiferromagnets.[18] Recently these effects have also been observed in the paramagnetic phase of $CeAl_2$.[7] It is interesting to investigate similar effects for SAW. For the Faraday-effect geometry [$\vec{k}$ parallel $\vec{B}$, case (c) above] the analogy breaks down, because the rotation of the polarization vector $\vec{U}$ cannot be continued into the upper half plane. Indeed for this geometry we could not observe any amplitude modulation for the SAW pulse. We only observed a broadening of the SAW pulse for high magnetic fields. For the Cotton-Mouton-Voigt geometry the analogy with the bulk case, however, holds. Consider the different magnetic field dependence of the SAW velocity in the two geometries (a) and (b). In both cases we have $\vec{k}$ perpendicular to $\vec{B}$. If one tilts the magnetic field 45° to the normal of the surface both SAW-modes are af-

fected and because the SAW velocities are different for the two modes one can expect an amplitude modulation. Clear-cut examples for such a magnetic field induced SAW birefringence are shown in Fig. 6. Especially for 25 MHz we observed a 100%-amplitude modulation, whereas for 13 MHz it was much smaller. Note that we did not observe any magnetic field dependence of the echo amplitude for the cases (a) and (b) alone.

The experimentally observed phase difference per unit length

$$\frac{\Phi}{l} = \omega\left(\frac{1}{v_a} - \frac{1}{v_b}\right) \tag{5}$$

is plotted in Fig. 7 for the two frequencies. In doing this we had to use an effective length l which was taken from the middle of the generating transducer to the middle of the receiving transducer for the direct pulse. For the first reflection from the corner we had to add twice the distance of the middle of the receiver to the corner. Consecutive maxima and minima have a phase difference $\Phi = \pi$.

Equation (5) was also used to determine a calculated Φ/l from the previously measured velocities in the two geometries. The agreement between experiment and calculation is not perfect as shown in Fig. 7. Unlike the case of the Cotton-Mouton effect for bulk waves,[7] where the frequency dependence of the phase Φ was linear [Eq. (5)], we find here for the SAW interference effect a different frequency dependence. By choosing an effective length for each frequency one could get better agreement between experiment and calculation. The reason for this discrepancy must lie in the finite size of the transducers (see Fig. 1). One has to consider additional amplitude modulation in this region. As one measures an integrated response over the finite comb structure, additional interference effects may occur, so that we see different oscillations than expected from Eq. (5). A detailed quantitative study of these various interference effects will be published elsewhere.

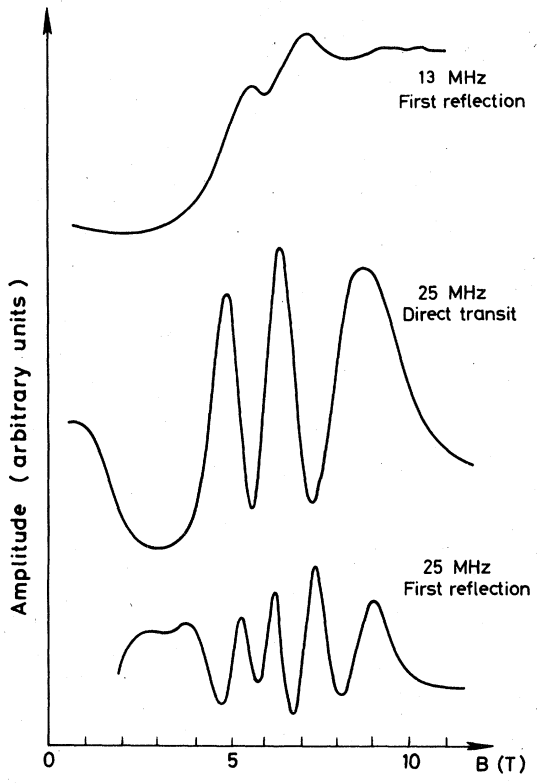

FIG. 6. Typical recorder traces for amplitude modulation in $CeAl_2$ as a function of magnetic field in Cotton-Mouton-Voigt geometry.

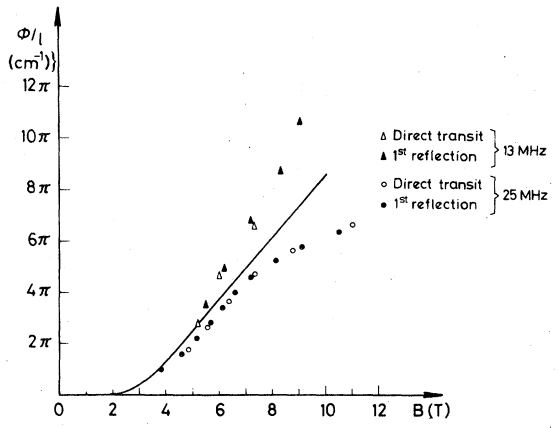

FIG. 7. Φ/l (B) for $CeAl_2$ for 13 and 25 MHz. The calculation using bulk data is given by the full line. Φ/l axis normalized to 25-MHz data.

V. CONCLUSIONS

We have performed surface acoustic wave experiments to study elastic and magnetoelastic effects in the paramagnetic phases of $CeAl_2$ and SmSb. This is the first time that SAW were used for investigating the temperature and field dependence of SAW velocities and related interference effects.

The important results can be briefly stated as follows:

(a) The temperature dependence of the SAW velocity can be explained by the theory of Rayleigh waves, applied to elastic anisotropic materials.[13] As in the case of bulk waves, crystal field effects were seen also for SAW.

(b) The magnetic field dependence of the SAW velocity was studied in detail for $CeAl_2$ at 4.3 K for various directions of the magnetic field. The resem-

blance of the data with the corresponding magnetic field dependence of the bulk c_{44} mode is very strong. This is due to the fact that the particle motion in a SAW is very close to the corresponding particle motion of a c_{44} mode (except for penetration effects and a small ellipticity). Our SAW results can be interpreted with the strain susceptibilities, in a manner analogous to the bulk case.

(c) An effect due to rotationally invariant magnetoelastic interactions could be isolated for two field dependent modes and agreement with a corresponding theory was found.[8]

(d) Because of the strong dependence of SAW velocities on the magnetic field direction, magnetoacoustic birefringence experiments are feasible. The SAW analogy of the magnetoacoustic Cotton-Mouton-Voigt effect[18] was observed in $CeAl_2$. This effect results in an amplitude modulated interference pattern of two normal modes of SAW. Agreement with theoretical predictions is not so good because of further destructive interference of SAW due to the finite size of the transducers.

For the present investigation we took two well characterized substances SmSb and $CeAl_2$, because we had single crystals of large enough sizes. To test our single-ion theory of SAW, substances with pure single-ion properties would have been more desirable, as, e.g., TmSb.[17] However, large enough single crystals of this substance were not available.

A comment should be made about the absence of a magnetic field dependence in SmSb and the rather large field dependence of SAW velocity in the case of $CeAl_2$. Both magnetic field dependences were measured at helium temperatures, i.e., close to T_N. We think that important fluctuation effects are responsible for the absence and the strong presence of velocity effects in the two cases. It was shown above that in $CeAl_2$ single-ion effects account only for about 50% of the measured field dependent effect. Fluctuation effects seem to balance single-ion effects in SmSb and enhance them in $CeAl_2$. Any quantitative calculations of such fluctuation effects are difficult, because the spin structure in the ordered phases are either not known (SmSb) or very complicated[19] ($CeAl_2$).

The observed interference effect in $CeAl_2$ for the Cotton-Mouton-Voigt geometry is a discovery with considerable potential. Detailed investigations as to the effect of finite transducer size on the phase relation of the interference pattern are under way. They give qualitatively the correct interpretation of the disagreement between experiment and calculation shown in Fig. 7.

Because in a SAW the particle motion is confined to the plane given by surface normal $\hat{n}$ and propagation direction $\vec{k}$, other interference effects are possible. For example, by placing the magnetic field in between $\hat{n}$ and $\vec{k}$ an interference pattern between the split modes of cases (a) and (c) is possible in principle, although for our frequencies and $CeAl_2$ the effect is very small. But, in principle, rotationally invariant magnetoelastic interactions could be observed also as an interference effect in the case of SAW and appropriate materials.

ACKNOWLEDGMENTS

We have enjoyed many helpful discussions with R. E. Camley and P. Fulde. We would like to thank P. Fulde for suggesting these experiments. A. Müller gave expert technical assistance. This work was supported by the Sonderforschungsbereich 65 Frankfurt-Darmstadt.

[1]See *Topics in Applied Physics,* edited by A. A. Oliner (Springer-Verlag, New York, 1978), Vol. 24.
[2]A. A. Maradudin and D. L. Mills, Ann. Phys. (N.Y.) 100, 262 (1976).
[3]E. Krätzig, Solid State Commun. 9, 1205 (1971).
[4]J. R. Sandercock, Solid State Commun. 26, 547 (1978).
[5]L. Bjerkan and K. Fossheim, Solid State Commun. 21, 1147 (1977).
[6]M. E. Mullen, B. Lüthi, P. S. Wang, E. Bucher, L. D. Longinotti, J. P. Maita, and H. R. Ott, Phys. Rev. B 10, 186 (1974).
[7]B. Lüthi and C. Lingner, Z. Phys. B 34, 157 (1979).
[8]R. E. Camley and P. Fulde (unpublished).
[9]J. de Klerk and E. F. Kelly, Rev. Sci. Instrum. 36, 506 (1965).
[10]K. Dransfeld and E. Salzmann, in *Physical Acoustics,* edited by W. P. Mason and R. N. Thurston (Academic, New York, 1970), Vol. VII.
[11]T. J. Moran and B. Lüthi, Phys. Rev. 187, 710 (1969).
[12]See, e.g., L. D. Landau and E. M. Lifshitz, *Theory of Elasticity* (Pergamon, New York, 1959).
[13]R. Stoneley, Proc. R. Soc. London Ser. A 232, 447 (1955).
[14]B. Lüthi, in *Magnetism and Magnetic Materials—1976,* edited by J. J. Becker and G. H. Lander, AIP Conf. Proc. No. 34 (AIP, New York, 1976), p. 7.
[15]P. Fulde, in *Handbook on the Physics and Chemistry of Rare Earths,* edited by K. A. Gschneidner and L. Eyring (North-Holland, Amsterdam, 1979), Chap. 17.
[16]V. Dohm and P. Fulde, Z. Phys. B 21, 369 (1975).
[17]P. S. Wang and B. Lüthi, Phys. Rev. B 15, 2718 (1977).
[18]See B. Lüthi, in *Dynamical Properties of Solids,* edited by G. K. Horton and A. A. Maradudin (North-Holland, Amsterdam, 1980), Vol. III.
[19]S. M. Shapiro, E. Gurwitz, R. D. Parks, and L. C. Kupferberg, Phys. Rev. Lett. 43, 1748 (1979).